iScience, Volume *27*

Supplemental information

Extracellular matrix protein composition dynamically changes during murine forelimb development

Kathryn R. Jacobson, Aya M. Saleh, Sarah N. Lipp, Chengzhe Tian, Audrey R. Watson, Callan M. Luetkemeyer, Alexander R. Ocken, Sabrina L. Spencer, Tamara L. Kinzer-Ursem, and Sarah Calve

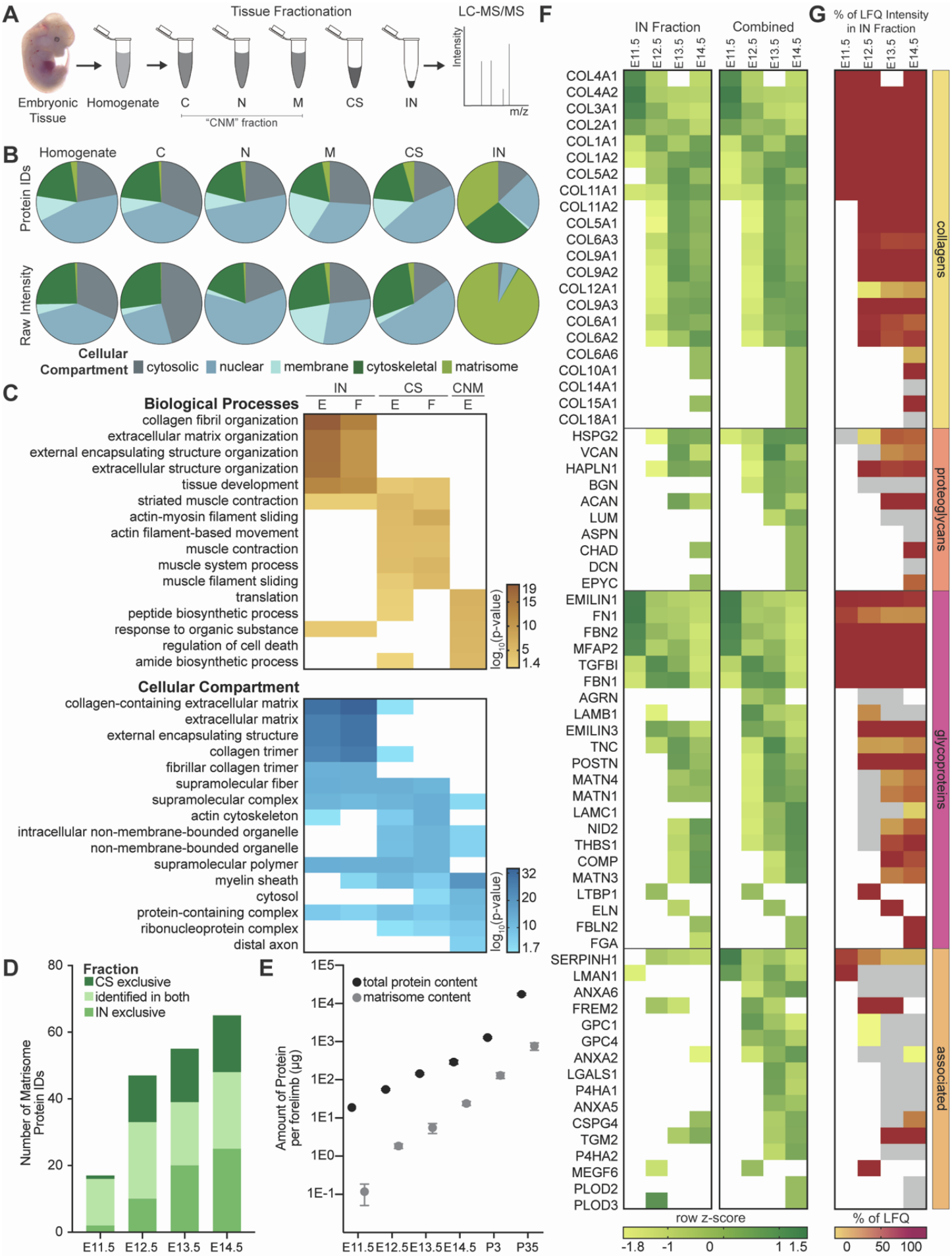
A
Tissue Fractionation
LC-MS/MS
Embryonic Tissue
Homogenate
C
N
M
CS
IN
"CNM" fraction
Intensity
m/z
B
Homogenate
C
N
M
CS
IN
Protein IDs
Raw Intensity
Cellular Compartment
cytosolic
nuclear
membrane
cytoskeletal
matrisome
C
Biological Processes
IN
CS
CNM
E
F
collagen fibril organization
extracellular matrix organization
external encapsulating structure organization
extracellular structure organization
tissue development
striated muscle contraction
actin-myosin filament sliding
actin filament-based movement
muscle contraction
muscle system process
muscle filament sliding
translation
peptide biosynthetic process
response to organic substance
regulation of cell death
amide biosynthetic process
log10(p-value)
19
15
10
5
1.4
Cellular Compartment
collagen-containing extracellular matrix
extracellular matrix
external encapsulating structure
collagen trimer
fibrillar collagen trimer
supramolecular fiber
supramolecular complex
actin cytoskeleton
intracellular non-membrane-bounded organelle
non-membrane-bounded organelle
supramolecular polymer
myelin sheath
cytosol
protein-containing complex
ribonucleoprotein complex
distal axon
log10(p-value)
32
20
10
1.7
D
Fraction
CS exclusive
identified in both
IN exclusive
Number of Matrisome Protein IDs
80
60
40
20
0
E11.5
E12.5
E13.5
E14.5
E
total protein content
matrisome content
Amount of Protein per forelimb (µg)
1E5
1E4
1E3
1E2
1E1
1E0
1E-1
E11.5
E12.5
E13.5
E14.5
P3
P35
F
IN Fraction
Combined
E11.5
E12.5
E13.5
E14.5
COL4A1
COL4A2
COL3A1
COL2A1
COL1A1
COL1A2
COL5A2
COL11A1
COL11A2
COL5A1
COL6A3
COL9A1
COL9A2
COL12A1
COL9A3
COL6A1
COL6A2
COL6A6
COL10A1
COL14A1
COL15A1
COL18A1
HSPG2
VCAN
HAPLN1
BGN
ACAN
LUM
ASPN
CHAD
DCN
EPYC
EMILIN1
FN1
FBN2
MFAP2
TGFBI
FBN1
AGRN
LAMB1
EMILIN3
TNC
POSTN
MATN4
MATN1
LAMC1
NID2
THBS1
COMP
MATN3
LTBP1
ELN
FBLN2
FGA
SERPINH1
LMAN1
ANXA6
FREM2
GPC1
GPC4
ANXA2
LGALS1
P4HA1
ANXA5
CSPG4
TGM2
P4HA2
MEGF6
PLOD2
PLOD3
row z-score
-1.8
-1
0
1
1.5
G
% of LFQ Intensity in IN Fraction
E11.5
E12.5
E13.5
E14.5
collagens
proteoglycans
glycoproteins
associated
% of LFQ
0
50
100

Figure S1. Proteomic analysis of fractionated murine embryonic tissues confirmed enrichment of matrisome in the insoluble (IN) fraction. Related to Figures 1 and 2. (A) Experimental workflow combining tissue fractionation with LC-MS/MS to investigate the ECM protein composition of embryonic tissues. **(B)** The distribution of protein IDs and raw protein intensities in the homogenate and fractions of E12.5 murine embryos (average, n=2 biological replicates), revealed a significant increase in percent matrisome in the IN pellet, compared to the homogenate and other fractions (p<0.001, one-way ANOVA). **(C)** The top 5 significant "Cellular Component" and "Biological Process" terms generated by GO analysis of the 50 most abundant proteins within each CNM (combined C, N and M), CS and IN fraction of E14.5 whole embryos and forelimbs indicated successful enrichment of ECM-related GO terms in the IN fraction. **(D)** The majority of ECM proteins were identified in both the CS and IN fractions of E11.5-E14.5 forelimbs. **(E)** The average amount of total protein (black) and matrisome (grey) in one forelimb (average and standard deviation of n=3). **(F)** Row z-scores were calculated for the normalized LFQ intensities in the IN fraction (left) and combined intensities (right). By combining CS and IN intensities, the number of ECM protein identifications increased, but overall matrisome dynamics did not change. For heat map analysis, white boxes signify proteins not identified in $n \geq 2$ biological replicates. **(G)** The percentage of combined LFQ intensity from the IN fraction was protein and timepoint specific. Percentages were plotted as the average across biological replicates (n=3). Grey boxes denote protein intensities identified exclusively in the CS fraction.

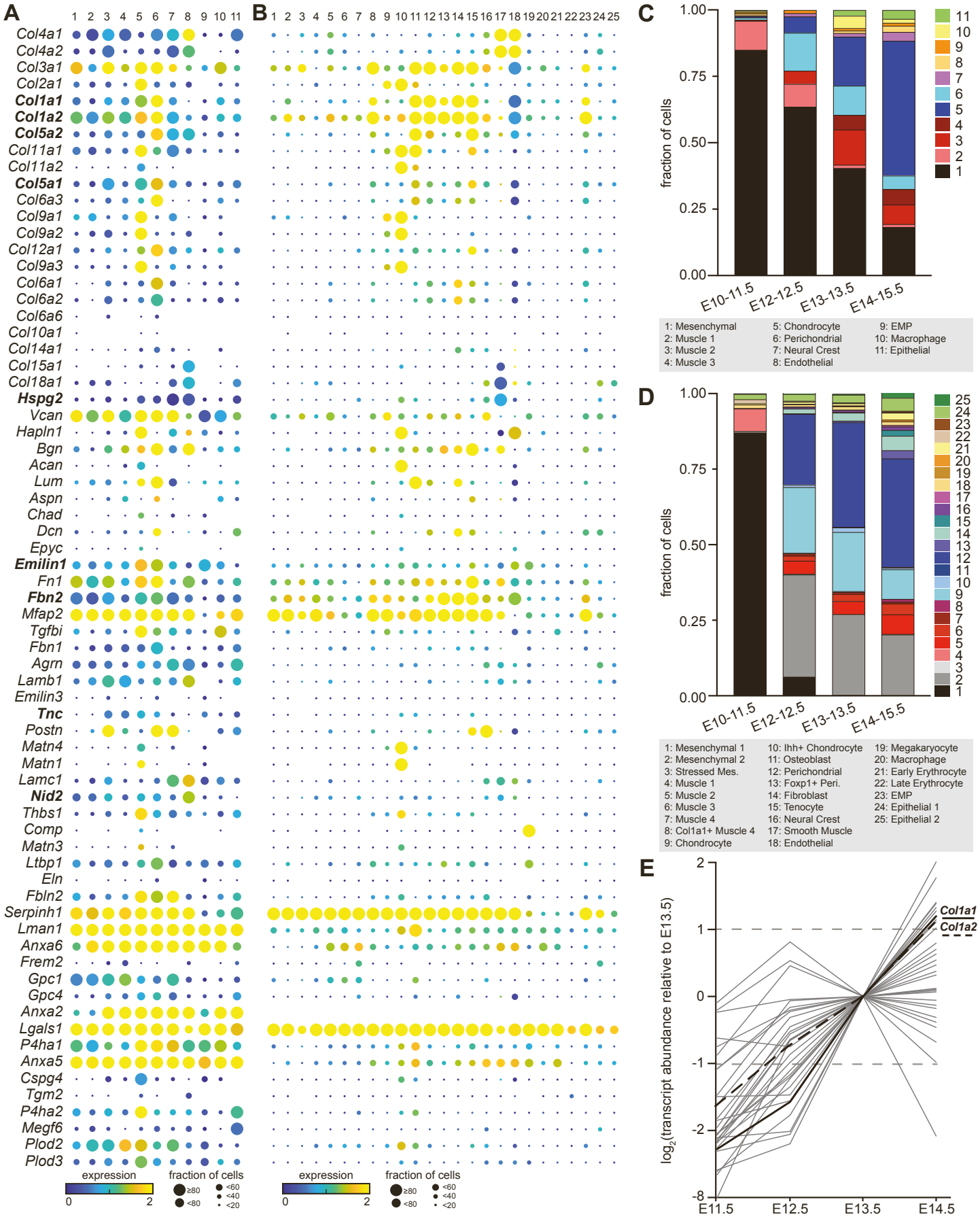

Figure S2. ECM expression by different cell types of the developing forelimb as identified via scRNA-sequencing. Related to Figure 2. Analysis of published scRNA-seq data[3] provided insight into the cell types that had the potential to

contribute to the synthesis of different ECM. (**A, B**) C1 Fluidigm (A) and 10X Genomics (B) scRNA-seq data sets were analyzed for ECM expression profiles and presented as dot plots to identify enriched genes in each cell type. Cell types were clustered and classified as described in [3]. Color indicates the $\log_2$(average expression + 1) and circle size represents the percentage of cells expressing that transcript. (**C, D**) Distribution of cell types identified as a function of age by C1 Fluidigm (C) or 10X Genomics (D). **(E)** Gene expression levels during limb development (E11.5-E14.5) for the nascent ECM identified 6-hpi between E13.5-E14.5 (**Figure 2D**), based on bulk RNA-seq data generated by [3]. The *x*-axis represents forelimb development, and the *y*-axis represents the average $\log_2$ fold-change of gene expression compared to the timepoint of injection, E13.5 ($n \geq 2$). Dashed horizonal lines depict fold-change of +/-2.

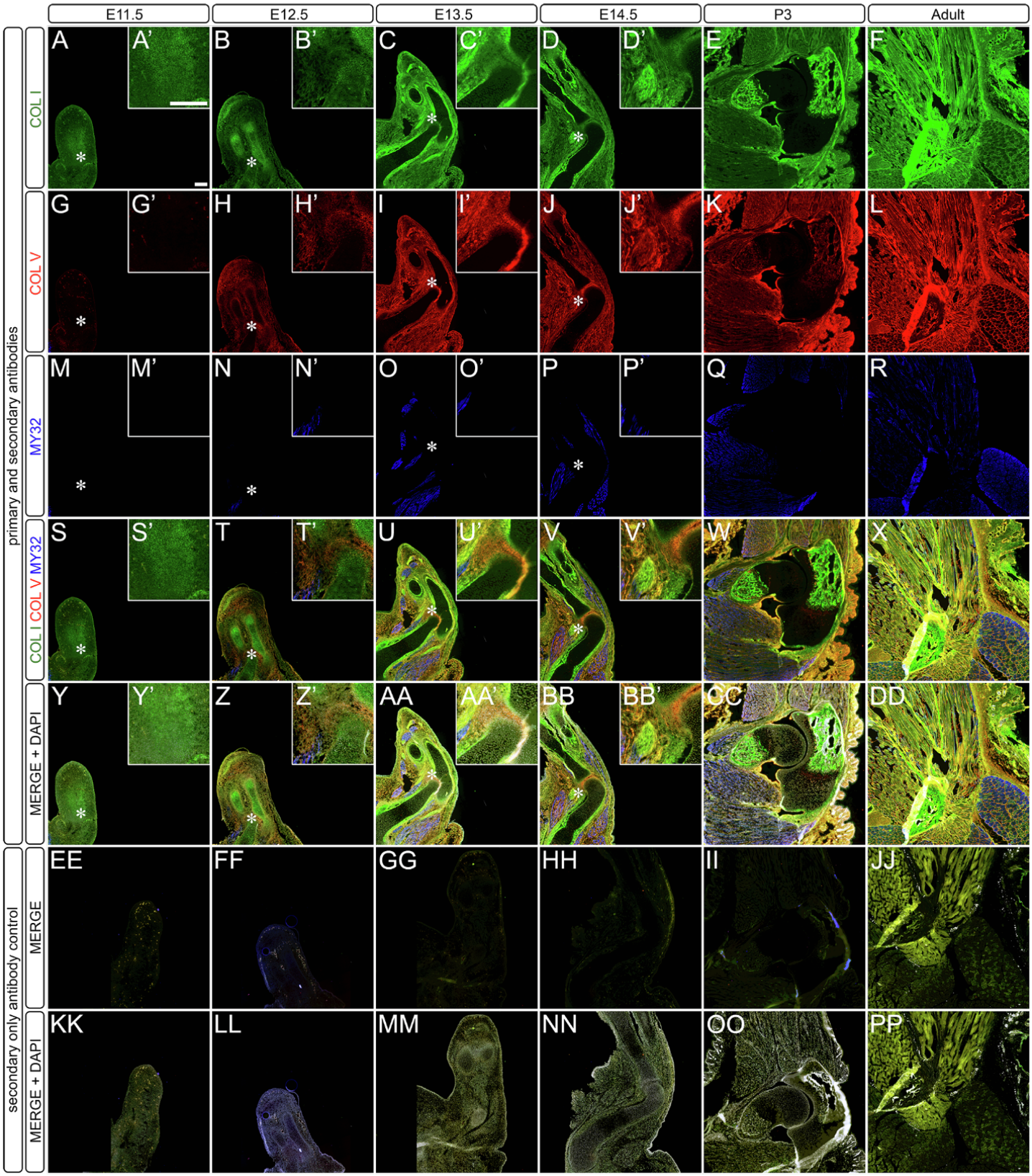

Figure S3. Spatiotemporal distribution of collagens, type I and V, during forelimb development show differential patterning of proteins. Related to Figure 4. (A-DD) Cryosections from E11.5 – E14.5, P3 and adult were stained with antibodies against: **(A-F, A'-D')** type I collagen (COL I; green); **(G-L, G'-J')** type V collagen (COL V; red); **(M-R, M'-P')** myosin heavy chain, a marker for differentiated skeletal muscle (MY32; blue); **(S-X, S'-V')** merge (green, red, blue); and **(Y-DD, Y'-BB')** merge with DAPI (grey). **(EE-PP)** Secondary antibody only negative controls: **(EE-JJ)** merge; and **(KK-PP)** merge with DAPI. Insets (indicated with ') are a 3× enlargement of the region containing the nascent elbow (*) for E11.5-E14.5. Scale bars=200 μm.

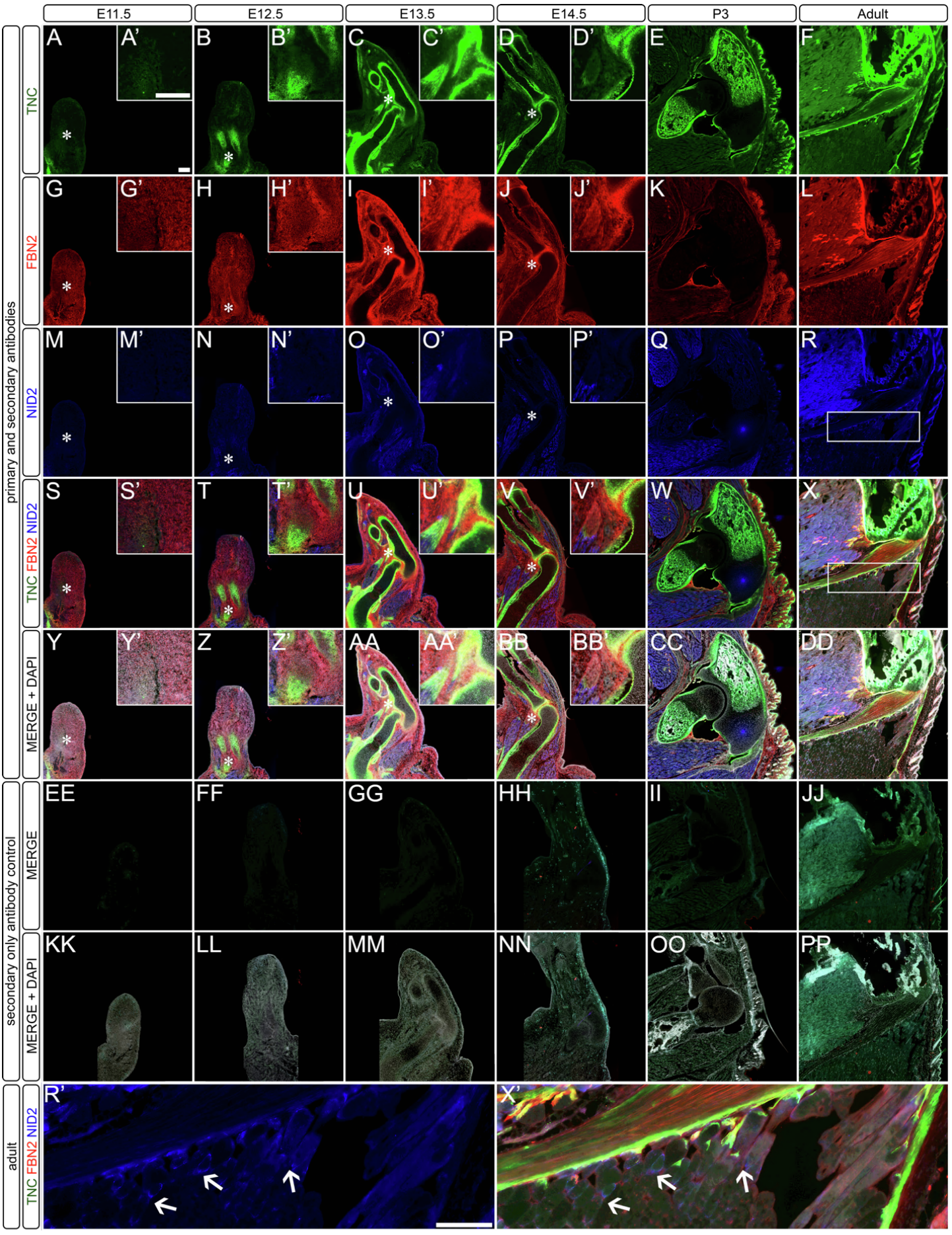
E11.5
E12.5
E13.5
E14.5
P3
Adult
primary and secondary antibodies
TNC
FBN2
NID2
TNC FBN2 NID2
MERGE + DAPI
secondary only antibody control
MERGE
MERGE + DAPI
adult
TNC FBN2 NID2
A
A'
B
B'
C
C'
D
D'
E
F
G
G'
H
H'
I
I'
J
J'
K
L
M
M'
N
N'
O
O'
P
P'
Q
R
S
S'
T
T'
U
U'
V
V'
W
X
Y
Y'
Z
Z'
AA
AA'
BB
BB'
CC
DD
EE
FF
GG
HH
II
JJ
KK
LL
MM
NN
OO
PP
R'
X'

Figure S4. Spatiotemporal distribution of tenascin-C, fibrillin-2 and nidogen-2 during forelimb development show differential patterning of proteins. Related to Figure 4. (A-DD) Cryosections from E11.5 – E14.5, P3 and adult were stained with antibodies against: **(A-F, A'-D')** tenascin-C (TNC; green); **(G-L, G'-J')** fibrillin-2 (FBN2; red); **(M-R, M'-P')** nidogen-2 (NID2; blue); **(S-X, S'-V')** merge (green, red, blue); and **(Y-DD, Y'-BB')** merge with DAPI (grey). **(EE-PP)** Secondary antibody only negative controls: **(EE-JJ)** merge; and **(KK-PP)** merge with DAPI. Insets (indicated with ') **(R')** NID2 and **(X')** TNC/FBN2/NID2 merge channels showed punctate staining (arrow) of NID2 in the adult. White box in **(R)** and **(X)** highlighted the inset location. Other insets are a 3× enlargement of the region containing the nascent elbow (*) for E11.5–E14.5. Scale bars=200 μm.

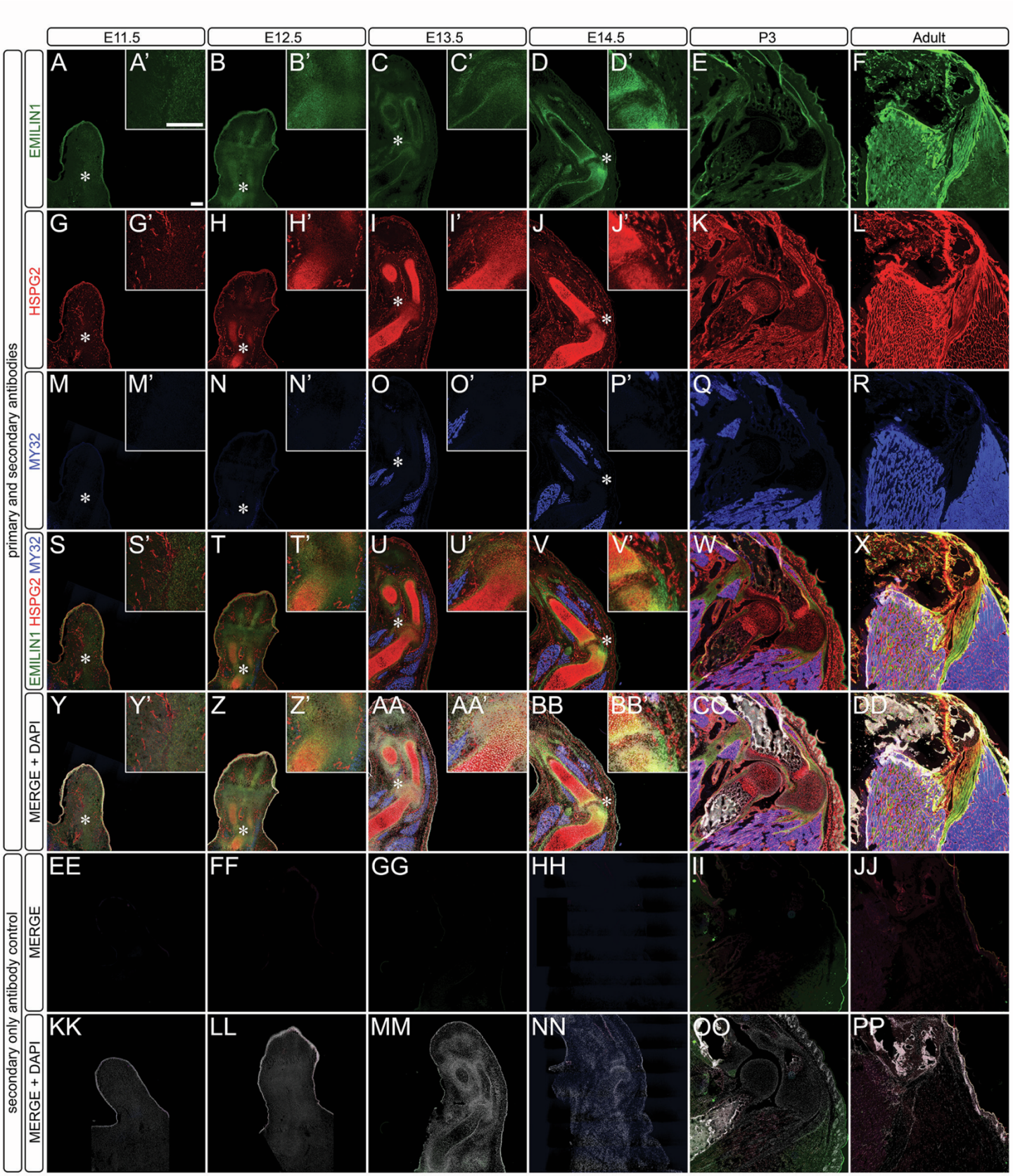

Figure S5. Spatiotemporal distribution of elastin microfibril interfacer 1 (EMILIN1) and perlecan (HSPG2) during forelimb development show differential patterning of proteins. Related to Figure 4. (A-DD) Cryosections from E11.5-E14.5, P3 and adult were stained with antibodies against: **(A-F, A'-D')** EMILIN1 (green); **(G-L, G'-J')** perlecan (HSPG2; red); **(M-R, M'-P')** myosin heavy chain, a marker for differentiated skeletal muscle (MY32; blue); **(S-X, S'-V')** merge (green, red and blue); and **(Y-DD, Y'-BB')** merge with DAPI (grey). **(EE-PP)** Secondary antibody only negative controls: **(EE-JJ)**

merge; and **(KK-PP)** merge with DAPI. Insets (indicated with ’) are a 3× enlargement of the forelimb containing the nascent elbow for E11.5-E14.5 at the location indicated with *. Scale bars=200 μm.